Geoderma 305 (2017) 363–373

Contents lists available at ScienceDirect

Geoderma

journal homepage: www.elsevier.com/locate/geoderma

Selenium and salt mobilization in wetland and arid upland soils of Pariette Draw, Utah (USA)

Colleen P. Jones[a,*], Paul R. Grossl[b], Michael C. Amacher[c], Janis L. Boettinger[b], Astrid R. Jacobson[b], John R. Lawley[b]

[a] Utah State University - Plants, Soils and Climate Department, 320 N. Aggie Blvd, Vernal, UT 84078, USA
[b] Utah State University - Plants, Soils and Climate Department, 4820 Old Main Hill AGS 348, Logan, UT 84322-4820, USA
[c] Rocky Mountain Research Station, U.S. Forest Service, 860 N. 200 E. Logan, UT 84321, USA

ARTICLE INFO

Handling editor: Edward A Nater

Keywords:
Selenium
Salinity
Wetlands
Arid land
Pariette Wetlands
Pariette Draw

ABSTRACT

Selenium (Se) mobilization in the soils of the Pariette Draw and subsequent accumulation into the Pariette Wetlands threaten wildlife. To gain a better understanding of the soil biogeochemistry of Se in the draw, the physical and chemical properties for two soils in the Pariette Draw located in eastern Utah were compared: one a formerly arid soil (elevation 1448 m) that was flooded following the creation of the wetlands in 1975, and the other an arid soil (elevation 1467 m). The soils were analyzed, and the influence of inundation by irrigation return water of Pariette Draw of Utah was assessed to obtain a better understanding of soil Se and salts in this system. It appears that Se mobility, especially in the wetlands soil, is associated with the distribution of soluble salts in the soil profile. Due to a fluctuating water table caused by a deluge of irrigation return water and high evapotranspiration rates coupled with low precipitation, capillary migration is the dominant mechanism driving the distribution and accumulation of salts and soluble Se in the upper horizons (Byz) of the wetlands soil. The distribution of soluble salts and Se in the upland soil is typical of a downward gravity-driven hydrology process. Gypsum solubility regulated sulfate levels within the Byz horizons of the wetlands soil. We surmise that soluble Se is regulated by the solubility of a sodium selenate sulfate coprecipitate. It appears that the relatively low concentration of Se in the local Pariette Wetlands soil is not the source and cause of Se responsible for adversely affecting wildlife in the wetlands.

1. Introduction

Pariette Wetlands is the United States Department of the Interior Bureau of Land Management's (USDI BLM) largest wetlands development in Utah, and was created to provide wildlife habitat in an arid environment. The Pariette Wetlands is an arid land oasis in the Uinta Basin located in northeastern Utah and part of the Pariette Draw (Fig. 1). The primary land uses within the Pariette Draw (about 56 km southwest of Vernal, Utah) are irrigated hay, pasture, and livestock grazing. Used as rangeland, the area is also impacted by the oil and gas industry (Wingert and Adams, 2011). The wetlands comprises 23 ponds (Fig. 1), mainly filled with water diverted from the Duchesne River into the Pleasant Valley Canal from May to October for irrigation of farmland in Pleasant Valley. A few springs also provide a minimal source of water for the draw. As each pond fills, excess water flows over water control structures. After the last pond (Redhead Pond), approximately 1 km upstream from the mouth of the Pariette Draw, the draw flows into the Green River (Stephens et al., 1992; Wingert and Adams, 2011).

The Uinta Basin is a geologic structural basin, part of the physiographic region known as the Colorado Plateau. Formation of the Basin began during the Late Cretaceous Period, 70 to 80 million years ago, when the Uinta Arch rose slowly causing the Uinta Basin to subside. Then during the Eocene Epoch, 55 to 34 million years ago, a large saline lake call Lake Uinta helped form this basin (Stokes, 1986).

Sediment deposits during the Eocene Epoch formed the Uinta and Green River Formations (Stokes, 1986). These two formations compose most of the surface of Pariette Draw, and are known to be seleniferous in areas (Stephens et al., 1992). Following this formation, a system of great interior lakes was formed, and Lake Uinta was one of these lakes. Next, the Green River Formation accumulated fine clastic sediments. After the deposition of the Green River Formation, a sharp uplift of the Uinta Mountains occurred (Fike and Phillips, 1983). Then during Late Pleistocene Epoch, approximately 24,000 years ago, glacial retreat of the Unita Mountains caused alluvial deposits of the Uinta Formation

* Corresponding author.
E-mail addresses: colleen.jones@usu.edu (C.P. Jones), paul.grossl@usu.edu (P.R. Grossl), janis.boettinger@usu.edu (J.L. Boettinger), astrid.jacobson@usu.edu (A.R. Jacobson), john.lawley@usu.edu (J.R. Lawley).

http://dx.doi.org/10.1016/j.geoderma.2017.06.028
Received 27 January 2017; Received in revised form 17 May 2017; Accepted 26 June 2017

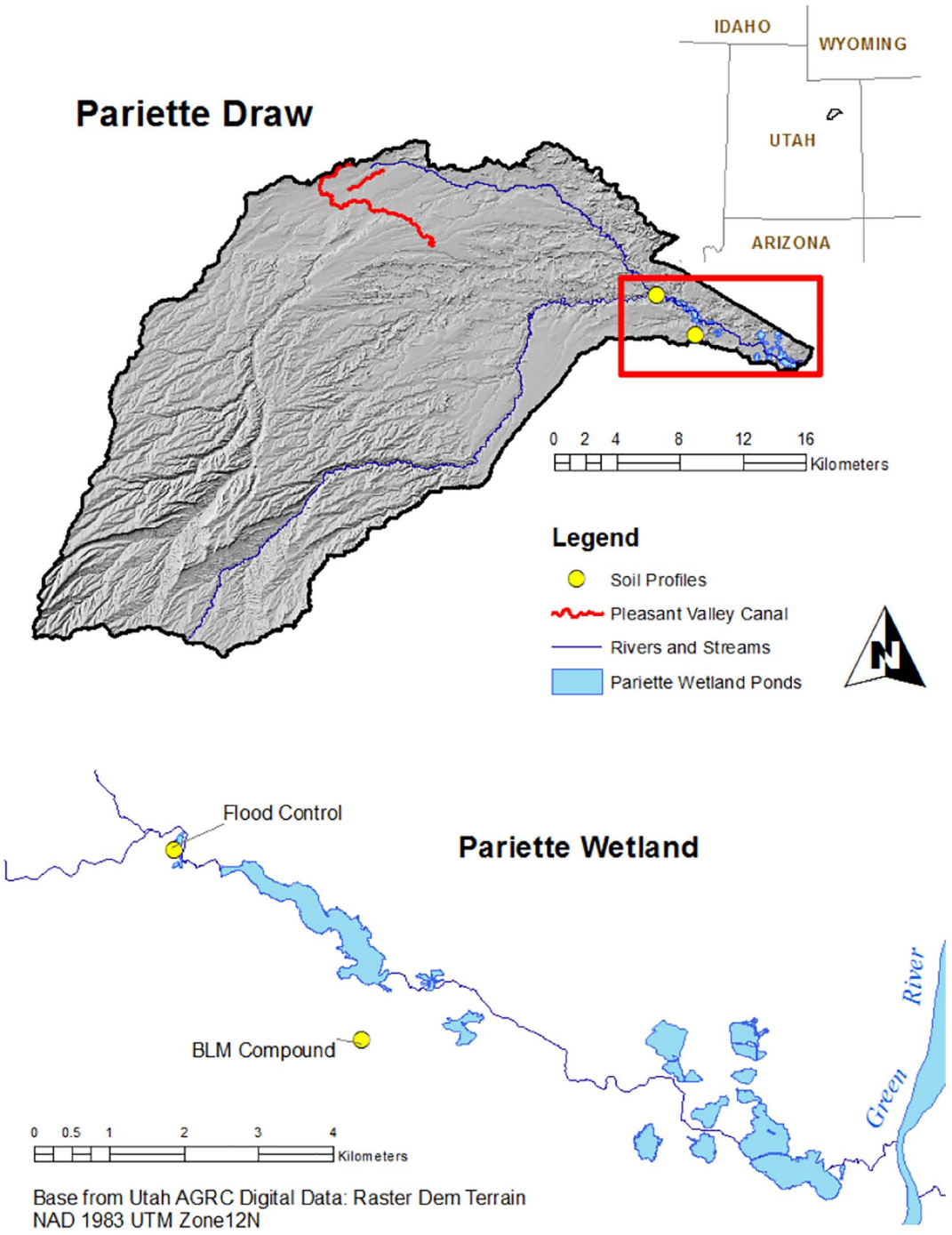

Fig. 1. Map of Pariette Draw and Pariette Wetlands study area (red box, expanded below), and locations of soil pedons (yellow circles). (For interpretation of the references to color in this figure legend, the reader is referred to the web version of this article.)

(Laabs et al., 2009).

Soil surveys completed in 1995 by the Natural Resources Conservation Service (NRCS) indicate that the soils at and near the wetlands are classified within the Aridisol and Entisol Soil Orders (Leishman et al., 2003). Soil parent material originates from lacustrine, fluvial and volcanic deposits. The area is a broad intermittent drainage with northwest to southeast descending slope. Unique landforms, considerable topographic relief, and deeply incised stream channels and washes characterize this area. The descriptive local topography is badlands, and the plant community is a mixture of desert shrub in the upland with cattails and rushes within the wetlands (Leishman et al., 2003). Map units from Soil Survey indicate that both sites are of the Motto-Rock outcrop complex. Motto series taxonomic classification is loamy, mixed, superactive, mesic, Lithic Natrargids (Leishman et al., 2003). The landform is a structural bench with well-drained soils formed from slope alluvium over residuum derived from shale and sandstone. Natrargids are Aridisols that have a natric horizon and do not have a pertrocalcic horizon within 100 cm of the soil surface (Soil Survey Staff, 2010). To date, NRCS has no detailed information listed about the salts and their association with each horizon.

In the Western United States, there has been increasing concern over Selenium (Se) contamination of public lands and waters resulting from irrigated agriculture and mining activities. Selenium is a naturally occurring element and is an essential trace element required for structure and function of certain proteins in animals (Hoffman, 2002; Winkel et al., 2012). In excess amounts, however, Se is known to cause

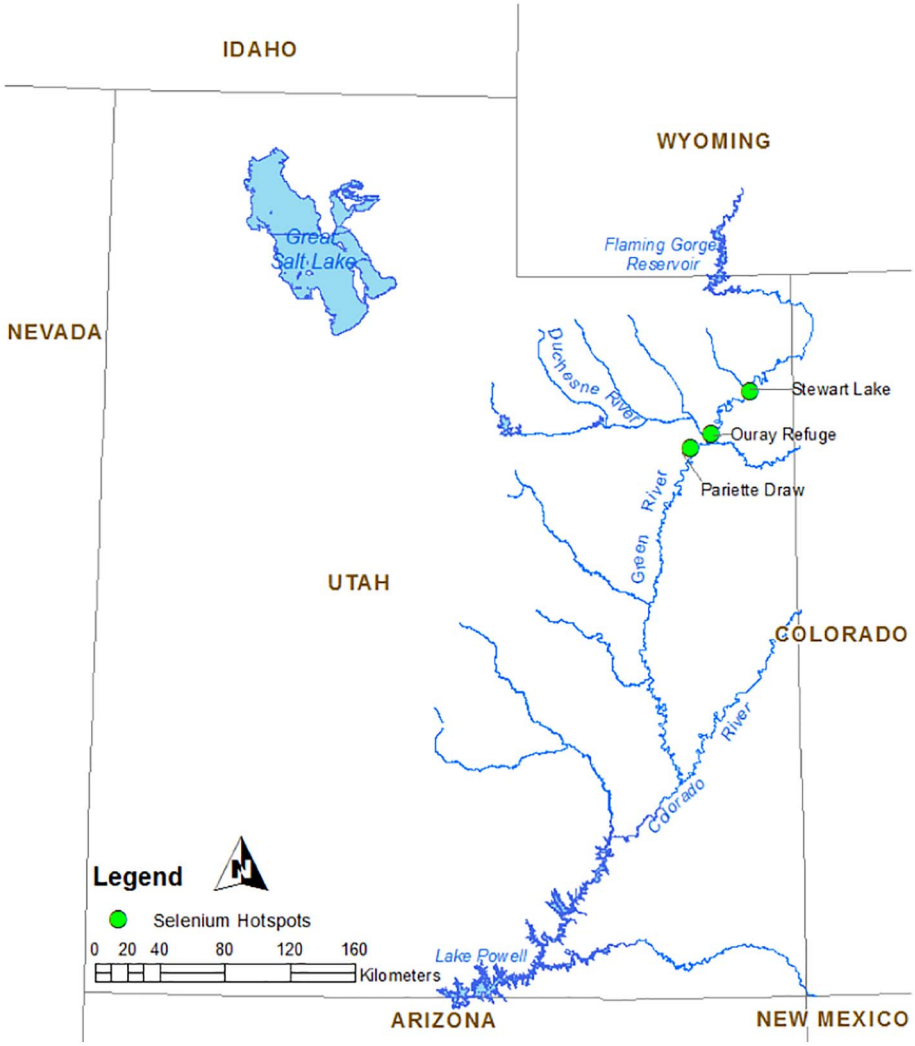

Fig. 2. Map of Selenium "hotspots" identified during the 1980's studies.

reproductive failures and abnormalities in egg-laying vertebrates such as birds, fish, amphibians, and reptiles (Hamilton, 2004; Lemly, 1985). Given the increasing occurrence of Se contamination throughout the world, it can be anticipated that this problem will continue to present challenges to land and wildlife managers (Lemly, 2002; Maher et al., 2010).

In the environment, Se is found in five metastable valence states: selenate, SeO_4^{2-}, (Se^{+6}); selenite, SeO_3^{2-}, (Se^{+4}); elemental Se (Se^0); selenides (Se^{-2}) and organic forms of Se (Maher et al., 2010). Under oxidized conditions, it is present as the oxyanions selenate and selenite. Selenate is the primary bioavailable form of Se, and, thus, the form that poses the greatest threat to the environment, especially under alkaline pH and aerobic conditions. As Se is reduced, selenite forms stable complexes with iron and aluminum, which are sorbed to soil and sediment particle surfaces and, consequently, are less mobile. However, both selenate and selenite, the oxidized form of Se, can occur in the same soil with the same conditions (Goldberg, 2011). Organic matter mineralization is associated with reduced redox potentials. At low redox potentials, Se forms insoluble elemental Se and metal selenides, which are unavailable to biota (Winkel et al., 2012). In its lowest oxidation state, Se forms metallic selenides (CuSe, $FeSe_2$, etc.), hydrogen selenide gas (H_2Se) or proteinaceous Se (selenomethionine or selenocysteine) (Presser, 1994). In aquatic ecosystems, cycling of Se occurs within the sediment pore waters, the water column and associated atmosphere. The major Se species in aquatic ecosystems can be categorized into four major groups: 1) inorganic Se, 2) volatile and methylated Se, 3) protein and amino acid Se, and 4) biochemical intermediates (Maher et al., 2010).

Since the early 1980s, high Se concentrations in agricultural drainage waters have been a major concern in the San Joaquin Valley, California (Seiler, 1995; Tanji et al., 1986). Here, subsurface irrigation drainage water containing high levels of Se was discharged and confined in Kesterson Reservoir, causing deformity of water bird embryos, ultimately leading to the reservoir closure in 1986 (Ohlendorf, 2002; Ohlendorf et al., 1986; Ohlendorf et al., 1988a; Ohlendorf et al., 1988b; Presser, 1994). Similarly, Se contamination has affecting some of Utah's waters that also serve as wildlife refuges. The middle Green River of the Uinta Basin area was identified as an area with significantly high Se contamination, and the Pariette Wetlands was identified as one of the three areas of concern in the basin (Peltz and Waddell, 1991; Stephens et al., 1992).

Selenium in Pariette Wetlands have been measured in water (1–16 μg/L), sediment (0.4–1.5 μg/g), plant (0.39–15.3 μg/g), invertebrate (3.2–10.6 μg/g), fish (4.4–10.9 μg/g) and bird (1.7–16.9 μg/L) tissues over the last 20 years at levels known to be hazardous to wildlife (Stephens et al., 1992; Wingert and Adams, 2011). Current recommended 4 day average chronic criterion for Se in water is 5 μg/L and 20 μg/L for acute criterion (U. S. EPA, 2014), and for sediment is 2 μg/g dry weight, according to Lemly (2002). High levels of Se exposure can cause reproductive failure and teratogenic deformities in oviparous organisms, such as birds and fish (Lemly, 1985; Chapman et al., 2010).

Selenium is a naturally occurring trace element associated with various geologic formations throughout the world; it is incorporated

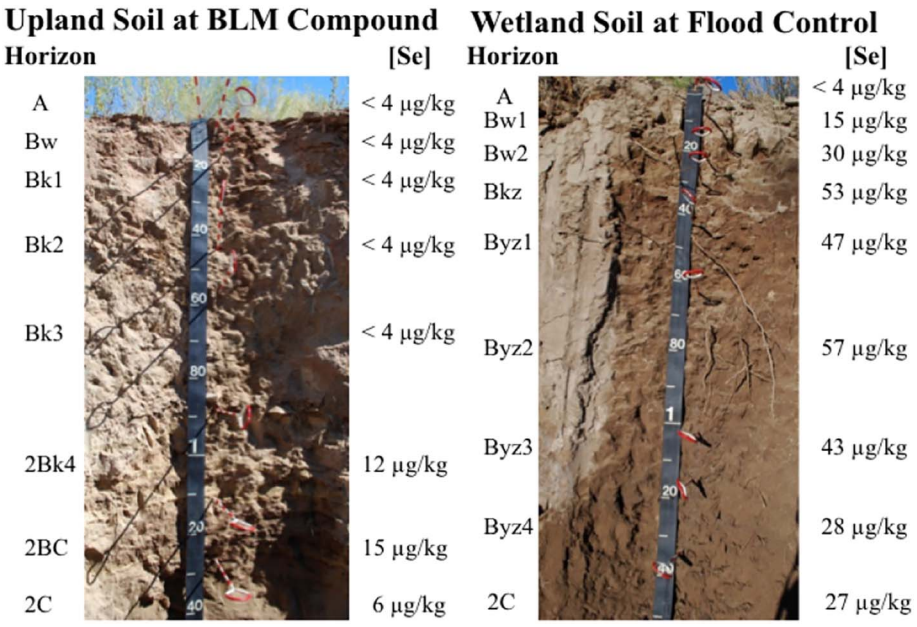

Fig. 3. Photos of soil profiles of Wetlands and upland soils of Pariette Draw, Utah.

into the geosphere in a wide range of geologic sources such as phosphate rocks, black shale, coal, and crustal rocks (de Souza et al., 1999; Maher et al., 2010). The main geologic sources of Se in the Pariette Draw are sedimentary rocks formed from ancient, organic rich, marine basins formed from sediments accumulated during the Upper Cretaceous Period (Pollard et al., 2007; Tuttle et al., 2014a, 2014b).

Processes such as physical and chemical weathering and soil genesis can mobilize sequestered Se from the lithosphere into the hydrosphere and atmosphere, causing Se to be more bioavailable in the environment (Maher et al., 2010). Both natural processes and anthropogenic factors mobilize Se. Potential natural processes that mobilize Se include chemical weathering either by snowmelt or rainfall run-off, leaching from saline soils, and upwelling of shallow groundwater. Potential anthropogenic causes include irrigation return flows, animal waste, oil/gas well pads, and non-point sources in the watershed (Wingert and Adams, 2011).

In the Western United States, wildlife deformities at Kesterson Reservoir and other sites led to investigations in the 1980's of Se environmental contaminations (Frankenberger and Engberg, 1998; Presser et al., 1994; Seiler et al., 2003). Similarly, the middle Green River area of the Uinta Basin, Utah, was identified as an area with significantly high Se contamination. Several studies conducted in the 1980's and since by the United States Geological Survey (USGS), United States Fish and Wildlife Service (USFWS), and the United States Bureau of Reclamation identified three areas of concern for Se contamination in the Middle Green River Basin (Peltz and Waddell, 1991; Stephens et al., 1992; Seiler et al., 2003; Tuttle et al., 2014a; Tuttle et al., 2014b).

The three areas of concern are Stewart Lake Waterfowl Management Area (SLWM), Ouray National Wildlife Refuge (ONWR), and Pariette Wetlands (Fig. 2) (Stephens et al., 1992). The source of Se contamination was believed to be from inflow of shallow ground water and surface water that flows through Mancos Shale known to be seleniferous (Stephens et al., 1992). The contaminated irrigation drain water that entered SLWM is currently diverted around SLWM and into the Green River (Naftz et al., 2008; Naftz et al., 2005). In 2002, a field study was conducted to assess passive remediation of Se-contaminated sediments by flooding and drying sediments to remove Se from the surface soils. Based on the Se flux rates of 0.65 mg/h/m^2, it would take 7 flooding cycles to meet the remediation goal of 4 µg/g in surface soils (Naftz et al., 2005; Rowland et al., 2003). Ouray National Wildlife Refuge's water samples ranged 9 to 93 µg/L. In 1987, Sheppard Bottom and Roadside Ponds of the ONWR were closed for a short period of time after discovery of deformed American coot embryos. Consequently, the ponds containing elevated levels of selenium were closed, drained and filled in with clean sediments (Stephens et al., 1988). In 2002, dikes in ONWR were rearranged to allow the Green River to naturally flood into Sheppard Bottom. Research is currently under investigation to assess the effectiveness of changes to dikes and management practices on Se bioaccumulation. Pariette Wetlands water samples ranged from 1 to 7 µg/L Se. Biota sampled during the same time contained Se concentrations intermediate between ONWR and SLWM. No deformed embryos were observed. However, the bioaccumulation factor of Se for Pariette Wetlands ranged 300 to 2200 times the Se concentration between the water samples and biota (Stephens et al., 1992).

After the 1980's studies (Stephens et al., 1992), most of the Se research in the Uinta Basin focused on SLWM (Naftz et al., 2008; Naftz et al., 2005; Rowland et al., 2003). Tuttle et al. (2014a, 2014b) in two companion papers investigated the geochemical cycles that occur during weathering of black shale and derived soil, and described the flux of salt and Se among shale, soil and aqueous phases in the same drainage of Pariette Wetlands.

Gypsum solubility mostly appears to govern the salt concentration in the Pariette Wetland soils (Tuttle et al., 2014b). Selenium is present predominately in immobile phases – adsorbed selenite, selenides and elemental Se - while mobile Se is selenate in a dynamic association with soil moisture and Na_2SO_4 salt, where soil solution Se concentrations are regulated by a “pseudo” equilibrium of soluble Se solid phases. (Tuttle et al., 2014a, 2014b) The objective of this study was to provide detailed physical and chemical properties of two soils, one from the arid upland and the other from the margin of the wetlands in the Pariette Draw. Our goal was to obtain a better understanding of the processes that regulate the distribution of Se in a typical arid soil compared to a soil affected by inundation of ground water in a created wetland setting. Insight into how inundation by water has impacted the Se distribution and form in the soil will be essential to understanding these processes that are applicable globally in other arid/created wetland settings. The information gained will lead to management strategies that will mitigate Se, thus minimizing the risk of Se toxicity to wildlife in those areas.

2. Materials and methods

2.1. Description of study area

Two different pedons of the Pariette Draw (Figs. 1 and 3) were

examined on September 17, 2011: one was located in somewhat poorly drained pedon inundated by irrigation return flow at the margin of the wetlands (1448 m), and the other was located in an upland area (1467 m) within the Pariette Draw. Sites were selected in stable undisturbed areas with representative native vegetation. The wetlands margin pedon was located downstream of the inlet to Pariette Wetlands below the Flood Control structure. The upland pedon was located upslope of the BLM compound building, and was not influenced by the inundation of water that created the current wetlands. The mean annual air temperature was 7.9 °C, and the maximum monthly average temperature for June, July and August was 30.5 °C. The minimum monthly average temperature for December, January, and February was −14.0 °C (Prono, 2008). Average annual precipitation and reference evapotranspiration at the nearby Myton, UT climate station for the period of 1993 to 2009 were 236 mm and 1180 mm, respectively. The aridity index (precipitation/evapotranspiration) for this site is 0.2. The soil moisture and soil temperature regimes were aridic and mesic, respectively.

2.2. Field methods

Soils were exposed by backhoe excavation to a depth of at least 150 cm. Genetic horizons were identified based on morphological features including color, texture, structure, effervescence with HCl, and visible salt crystals. Soils were described in the field and samples were collected from each genetic horizon (Soil Survey Staff, 2009).

2.3. Laboratory analysis

Soil samples were air-dried, crushed and passed through a 2-mm sieve to remove coarse fragments. Saturated paste extracts were obtained using an automatic vacuum extractor. Saturation percentages were measured before extraction by weighing and oven-drying part of the saturated paste and measuring the mass water content. Saturated paste extracts were analyzed for pH and electrical conductivity (ECe) (Soil Survey Staff, 2009). Soil ground to < 0.25 mm was analyzed for Calcium Carbonate Equivalent (CCE) (Fonnesbeck et al., 2013). Noncrystalline iron was extracted from the soil subsample using 0.2 M acid ammonium oxalate (Ross and Wang, 1993). Total elemental analysis including iron was determined on subsamples submitted to the United States Geological Survey (USGS) in Denver (Taggert, 2002). Total Se in the soils was determined by nitric-perchloric acid digestion followed by hydride generation atomic adsorption spectroscopy (Zasoski and Burau, 1977).

A subsample was taken from each saturated paste extract and submitted to the USGS for elemental analysis using inductively coupled plasma-atomic emission spectroscopy (ICP-AES) for all ions (Na^+, K^+, Ca^{2+}, Mg^{2+}, Cl^-, SO_4^{2-}, Al^{3+}, F^-, Mn^{2+}, SiO_2 and P) except Se, and hydride generation atomic absorption spectrometry (HG-AAS) for Se (Taggert, 2002). Sodium Adsorption Ratio (SAR) was calculated using the elemental analysis results (Soil Survey Staff, 2009).

2.4. Hydrogeochemical modeling

The chemical equilibrium model PHREEQC (v. 3) (Parkhurst and Appelo, 2013) with Minteq (v.4) data set was used to predict ion activities in the saturation extract solutions at 25 °C, saturated paste pH values, and redox potential associated with dry aerated (pe = 20.66–pH) or wet, aerobic soils (pe = 15-pH) (Azaizeh et al., 2003). The ECe was modeled by using PHREEQC (Parkhurst and Appelo, 2013) ionic strength output data for both soil profiles divided by Griffin and Jurinak (1973) activity coefficient (0.0127). Pearson's correlation test was used to test for significant correlation with ion concentrations in the extract paste and ECe.

The PHREEQC model was also used to calculate mineral saturation indexes for the minerals calcite ($CaCO_3$), gypsum ($CaSO_4 \cdot 2H_2O$), glauberite ($Na_2Ca(SO_4)_2$), and thenardite (Na_2SO_4) in the saturation extracts, and during soil pedon drying at 0.5x, 0.25x, and 0.125x, where x = saturation water content. Each mineral saturation index is defined by

$$SI = K_{sp}/IAP$$

where SI = mineral saturation index, K_{sp} = mineral solubility product (included in the MINTEQ database), and IAP = ion activity product in the saturation extract as calculated by PHREEQC.

2.5. X-ray diffraction analysis

Salts collected from the soil surface as well as clearly present white solids within the flood plain soil profile were analyzed by x-ray diffraction (XRD). The XRD was done using a Panalytical X'Pert Pro X-ray Diffraction Spectrometer with monochromatic Cu K-alpha radiation. High Score software was used to index peaks and identify minerals.

3. Results and discussion

3.1. Morphological and physical soil properties

The deep, somewhat poorly drained, wetlands-margin soil near the flood control structure was formed from alluvium and colluvium overlying colluvium derived from sandstone and mudstone of the Uinta Formation. This pedon occurred on an east-northeast-facing toeslope of a cliff with a slope gradient of 6%. The upland soil near the BLM Compound occurred on a south-southwest backslope of a ridge with a slope gradient of 8%. Soil moisture regime was typic aridic, and the soil temperature regime was mesic. The upland site supported a desert shrub community composed of native vegetation dominated by Indian rice grass (*Achnatherum hymenoides* (Roem. & Schult.) Barkworth), saltgrass (*Distichlis spicata* (L.) Greene), greasewood (*Sarcobatus vermiculatus* (Hook.) Torr.) and rabbit brush (*Ericameria nauseosa* (Pall. ex Pursh) G.L. Nesom & Baird). The wetlands-margin site in the riparian and flood plain zone consisted primarily of graminoids; common reed (*Phragmites australis* (Cav.) Trin. ex Steud.), cattails (*Typha domingensis* Pers. and *T. latifolia* L.), and rushes (*Schoenoplectus acutus* (Muhl. ex Bigelow) Á Löve & D. Löve, *Bolboschoenus maritimus* (L.) Palla, *Eleocharis palustris* (L.) Roem. & Schult., *Juncus arcticus* Willd. and *S. pungens* (Vahl) Palla).

Soil color is the most obvious feature of a profile, and may suggest chemical composition. The near-surface horizons of the wetlands-margin soil have a hue of 10YR and lower value, indicating the accumulation of organic matter turnover from the wetlands vegetation. At about 28 cm depth, chromas change from 3 to 2 (Table 1); change in chroma in the lower part indicated that the soil may be subject to saturation, facilitating the reduction and removal of Fe. Saturation of soils and sediments in the wetlands has caused the soluble salt to dissolve and mobilize, ultimately, precipitating in the horizons with visible gypsum veins (Byz1, Byz2, Byz3 and Byz4). The soils were moderately developed with subangular blocky structure in the solum, whereas the regolith was structureless single grain weathered sandstone (below 113 cm). The texture was sandy loam throughout the pedon except for sandy clay loam in the Byz4 horizon.

All horizons of the upland soil were 7.5YR and had chromas of 3, indicating that organic matter was low and the soil had not been subject to saturation. Several horizons had gravel lenses (Bk2 and Bk3), and alternating light and dark colored 1-cm thick sediment bands (2Bk4 and 2BCk). Carbonate coats around rock fragments and finely disseminated carbonates were present throughout profile (Table 1).

3.2. Soil forming processes and classification

The epipedon for the wetlands (Flood Control) pedon was ochric, and the diagnostic subsurface horizons were gypsic (41–131 cm) and

Table 1
Physical properties of wetland and upland soil profiles from Pariette Draw, Utah.

Horizon	Depth (cm)	Munsell color		Texture			Structure
		Dry	Moist	%RF	Class	%clay	
Wetland profile							
A	0–6	10YR 6/2	10YR 4/3	–	SL	8	SBK
Bw1	6–18	10YR 6/2	10YR 4/3	–	SL	18	SBK
Bw2	18–28	10YR 6/3	10YR 4/2	–	SL	17	SBK
Bkz	28–41	7.5YR 7/2	7.5YR 7/2	–	SCL	22	SBK
Bz1	41–62	7.5YR 6/2	7.5YR 4/2	1GR	SL	19	SBK
Bz2	62–101	7.5YR 6/2	7.5YR 5/2	1GR	SL	19	SBK
Bz3	101–113	7.5YR 6/2	7.5YR 4/2	3GR	SCL	23	SBK
Bz4	113–131	7.5YR 7/2	7.5YR 4/2	1GR	SL	17	SBK
2C	131–152	7.5YR 6/2	7.5YR 4/2	10GR & 60ST	STXSL	11	SGR
Upland profile							
A	0–4	7.5YR 7/3	7.5YR 4/3	2GR	SL	10	PL
Bw	4–14	7.5YR 6/2	7.5YR 5/3	25GR	GRCOSL	12	SBK
Bk1	14–41	7.5YR 5/3	7.5YR 4/3	35GR	GRVLCOS	6	SBK
Bk2	41–54	7.5YR 6/2	7.5YR 4/3	50GR	GRVLCOS	6	SBK
2Bk3	54–86	7.5YR 6/3	7.5YR 5/4	35GR	GRVLCOS	8	SBK
2Bk4	86–109	7.5YR 7/3	7.5YR 5/2	–	L	25	SBK
2BC	109–125	7.5YR 6/3	7.5YR 5/3	–	SIL	21	SBK
2C	125–154	7.5YR 6/4	7.5YR 5/3	–	FSL	12	MA

Notes - Texture: GR = Gravelly, ST = stony, SL = sandy loam, SCL = sandy clay loam, STXSL = extremely stony sandy loam, GRSOSL = gravelly coarse sandy loam, GRVLCOS = very gravelly coarse sandy loam, L = loam, SIL = silt loam, FSL = fine sandy loam.
Structure: SBK = subangular blocky, SGR = single grain, PL = platy, MA = massive.

sodic (6–152 cm). There were no other diagnostic characteristics, and the family particle size was fine-loamy (control section 25–100 cm). Based on these diagnostic characteristics, the family classification was fine-loamy, mixed, superactive, mesic Sodic Haplogypsids (Soil Survey Staff, 2010).

The diagnostic epipedon for the upland pedon (BLM Compound) was ochric, and the diagnostic subsurface horizons were cambic (14–86 cm), calcic (86–109 cm), and sodic (14–154). A genetic characteristic was a lithologic discontinuity of gravel lens with alternating light and dark sediment bands that occur at 86 to 109 cm. The family particle size was sandy-skeletal over loamy (control section 25–100 cm). The family classification was sandy-skeletal over loamy mixed, superactive, mesic Sodic Haplocalcids (Soil Survey Staff, 2010). Thus, despite their different landscape positions (wetland vs. upland) and differing soil texture, both pedons are Sodic Haplocalcids with significant salt-dominated genetic horizons, although with differing salt composition and distribution as discussed below.

3.3. Chemical properties

3.3.1. Soluble salts

The chemical properties of the upland and wetlands soils, especially with regard to the quantity and distribution of soluble salts in each profile, differed considerably (Table 2, Figs. 4a and 5a). Hydrology was the main factor responsible for the difference in accumulation and distribution of soluble salts between the two soil profiles. Comparison of ECe measured versus modeled gave good agreement with an R^2 value of 0.9958 (Fig. 6). The upland soil profile was typical of a well-drained, arid soil, where soluble salts and carbonate concentrations increased with depth due to a downward translocation of these materials transported via a gravity-driven hydrology. The ECe for the upland soil ranged from 0.54 to 2.62 dS/m, which is not extraordinarily high (Table 2 and Fig. 5a).

In contrast, the ECe values of the wetland-margin soil were one order of magnitude higher than the upland soil ranging from 3.27 to 27.4 dS/m (Table 2 and Figs. 4a and 5a). The wetland-margin had the highest ECe in mid layers of the soil profile (28 to 131 cm), indicating an upward translocation and accumulation of soluble salts via capillary migration due to alteration of the water table associated with inundation of irrigation return flow into the wetlands. The migration of the soluble salts to the surface was also influenced by the seasonal high evapotranspiration rates and low annual precipitation. The predominate ions of the saturated paste extracts were Na^+, Ca^{2+}, SO_4^{2-}, and Cl^-. A significant correlation ($p < 0.01$) existed between ECe and the soluble ions in the saturated paste extract, especially SO_4^{2-} ($r^2 = 0.96$). The extract SO_4^{2-} content in the Byz horizons of the wetlands soil was two orders of magnitude higher than in the soil.

Mineral saturation indexes in the saturation extracts of the soil profiles indicate that all horizons in both soil pedons are supersaturated with respect to calcite at full water saturation (Fig. 7). Calcareous soil solutions tend to be supersaturated with respect to calcite because of a kinetic constraint that tends to inhibit calcite precipitation (Amrhein et al., 1993). Despite this calcite precipitation inhibition, calcite formation does occur in time as indicated by the large amounts of CCE in both soil profiles (Figs. 4c and 5c).

Saturation extracts of the Byx horizons in the wetland soil pedon are in equilibrium with gypsum and as the soil profile dries, the soil solution would become supersaturated with respect to gypsum and would readily precipitate (Fig. 7). Wetland soil horizons are undersaturated with respect to glauberite at full water saturation, but the Byz horizons would become supersaturated with respect to this mineral as the soil profile water content decreased during drying (Fig. 7). Wetland soil horizons remain undersaturated with respect to thenardite at all calculated water contents, and would probably not form until the soil pedon was near fully air-dry.

In contrast with the wetland pedon, the upland pedon remained undersaturated with respect to gypsum, glauberite, and thenardite at all calculated water contents. Thus, these minerals would tend to dissolve during rainfall percolation and supply Na, Ca, and SO_4 to the wetland via subsurface water flow.

During soil genesis, soluble salts dissolve when in contact with water, translocate, and then precipitate as water recedes or evaporates. In the absence of a kinetic constraint, carbonates will precipitate first, followed by gypsum, and then sodium salts (Boettinger and Richardson, 2001). This distribution of salts in the wetland soil profile, as related to hydrology, followed a predicted sequence as proposed by the Hardie-Eugster model (Hardie and Eugster, 1970). The model predicts the following order of mineral formation upon concentrating the saline

Table 2
Chemical properties of soils from Pariette Draw, Utah.

Horizon	Depth (cm)	Sat. H_2O %	pHe	ECe (dS/m)	$CaCO_3$ equiv. %	Fe_{Total} %	Oxalate extract Fe (mg/kg)	SAR	Ca_e^{2+} (mg/kg)	K_e^{+} (mg/kg)	Mg_e^{2+} (mg/kg)	Na_e^{+} (mg/kg)	SO_{4e}^{2-} (mg/kg)	Se_e (μg/kg)	Se_{Total} (μg/kg)	Se_e Se_{Total}
Wetland																
A	0–6	30.8	8.10	3.27	4.64	1.4	228	10.60	27.60	11.67	2.74	218.69	172.49	< 3.50	34.5	0.10
Bw1	6–18	36.9	8.90	11.7	5.07	1.9	282	83.25	15.06	9.56	1.77	1284.84	1524.83	14.58	48.2	0.302
Bw2	18–28	36.4	9.10	18.2	4.93	1.8	398	144.36	10.51	9.31	2.95	2062.02	2552.97	30.22	76.5	0.39
Bkz	28–41	43.5	9.05	24.3	4.41	2.1	420	100.75	54.35	10.43	11.43	3138.98	4869.33	52.17	80.4	0.65
Byz1	41–62	37.3	8.59	25.5	3.31	2.0	320	62.96	126.85	7.98	16.15	2839.24	4775.60	46.64	91.5	0.51
Byz2	62–101	40.8	8.71	27.4	3.37	2.0	341	59.37	179.44	8.40	36.30	3344.13	6076.54	57.09	113.4	0.50
Byz3	101–113	36.0	8.74	27.4	3.56	1.9	337	52.79	169.15	7.85	39.59	2943.90	5722.25	43.19	115.6	0.37
Byz4	113–131	33.2	8.72	24.1	3.96	1.7	299	40.40	150.98	5.71	24.79	2037.44	5110.18	27.94	71.6	0.39
2C	131–152	38.6	8.71	20.5	5.11	1.8	287	43.51	160.36	5.95	37.79	2364.88	4714.31	27.17	66.0	0.41
Upland																
A	0–4	27.4	8.06	0.54	11.94	1.4	190	1.66	11.65	1.75	1.40	22.51	15.08	< 3.50	119.6	0.029
Bw	4–14	26.9	8.84	0.77	14.66	1.5	208	8.58	2.58	0.27	0.32	55.07	13.97	< 3.50	131.4	0.026
Bk1	14–41	32.2	8.83	1.19	9.25	1.3	254	19.52	1.51	0.29	0.32	101.46	85.35	< 3.50	97.8	0.036
Bk2	41–54	34.4	9.19	1.18	7.75	1.3	236	21.03	1.34	0.24	0.29	103.28	96.40	< 3.50	95.8	0.037
2Bk3	54–86	35.1	9.39	1.01	8.83	1.3	321	22.35	0.91	0.33	0.24	93.03	29.84	< 3.50	56.7	0.061
2Bk4	86–109	58.4	9.16	2.19	21.89	2.2	656	39.45	2.69	0.35	1.23	312.32	312.32	12.26	175.6	0.070
2BC	109–125	70.3	9.02	2.40	12.37	2.6	449	42.36	3.87	0.66	2.18	421.92	502.78	15.12	126.4	0.11
2C	125–154	49.0	9.03	2.62	6.92	1.9	400	30.31	4.17	0.47	2.06	303.94	409.34	5.54	70.5	0.08

Note: Sat. is abbreviation for saturation. Subscript e indicates measurements are made on saturated paste extract. < indicates that the concentration is below detection limit of the ICP-MS. In determining ratio of Se_e/Se_{Total} measurements below the detection limit, the detection limit is used.

pore water solutions: calcite, gypsum, glauberite, thenardite, and halite. First Ca is partially removed from solution with the formation of calcite. Additional Ca is removed along with sulfate when gypsum precipitates. Due to increasing Na levels, Ca and sulfate continue to precipitate in the form of glauberite, and ultimately nearly complete removal of Ca favors the formation of thenardite, followed very closely by halite. In the wetland soil, calcium carbonate, gypsum, glauberite, and thenardite, but not halite were measured by XRD. Calcium carbonate levels were lower in the Byz horizons (28 to 131 cm) (Fig. 4c) but higher (> 5% CCE) in the adjacent layers above and below the Byz horizons. A white precipitate could clearly be observed in the Byz horizons in the wetland profile, which was gypsum as identified by XRD. Likewise, the geochemical modeling indicated that gypsum ($CaSO_4 * 2H_2O$) solubility regulated the SO_4^{2-} levels in the Byz horizons of the wetlands soil. With the exception of the topmost surface soil layers, the pH values for both soils exceeded 8.5 and were most likely buffered by sodium carbonate. The upland soil on average had higher pH values than the wetlands soil. Surface salt crusts, which can be seen throughout the Pariette Draw, were collected and identified via XRD as being the mineral thenardite (Na_2SO_4). Thus, thenardite does form in these soils once full drying occurs at the soil surface as typically happens in the warm, dry summer months.

These same minerals (calcite, gypsum, and thenardite) were found to play an important role in regulating soluble salts in the Cretaceous Mancos Shale in the Colorado River Basin (Tuttle et al., 2014a). In their weathering model, during pedogenesis as shale disaggregated to form soil, bulk density decreased and porosity increased. Rainfall dissolved calcite and thenardite at or near the soil surface, infiltrated to about 1 m in depth, and precipitated gypsum during evapotranspiration, which enriched soil water in Na and residual sulfate. Transpiration of soil water to the soil surface and/or exposure of subsurface soil from slumping produced more thenardite.

3.3.2. Iron distribution

Iron solubility in both profiles also appeared to be regulated by hydrology, where the percent of demonstrated a similar distribution and accumulation pattern as the soluble salts (Table 2, Figs. 4d and 5d). This was confirmed by oxalate-extractable iron (Table 2, Figs. 4e and 5e). The fluctuating high water table in the wetland-margin soil resulted in fluctuating soil redox conditions and, subsequently, a dynamic zone of Fe dissolution and precipitation of ferric oxides in the Bkz and Byz horizons with Total Fe and oxalate-extractable Fe maxima at 28–41 cm (Bkz horizon). In the upland profile the percent total and oxalate-extractable Fe reached maxima lower in the profile at the Bk to BC horizon transition (86 to 125 cm indicating fluctuating redox conditions much deeper in its profile compared to the wetland profile.

3.3.3. Selenium distribution

Selenium distribution in the wetland and upland pedons is influenced by both soluble salts and iron chemistry (Fig. 3). In the wetland soil pedon, both total and soluble Se tended to reach a maximum in the Bkz and Byz horizons where there was an oxalate-extractable Fe peak and salts tended to accumulate as indicated by the ECe depth distribution (Table 2, Fig. 4a, e, and f). This is also the portion of the wetland pedon where CCE was at a minimum (Fig. 4c). Carbonate accumulation occurred above and below the areas of maximum accumulation of Fe oxides, soluble salts, and Se. In the upland soil total and soluble Se both had maxima closely associated where total and oxalate-extractable Fe had their maxima (Table 2, Fig. 5d, e, and f).

The high surface area ferric oxides are loosely able to retain selenite and sulfate as outer-sphere surface complexes (Dzombak and Morel, 1990). Stillings and Amacher (2004) showed that Se is strongly associated with Fe oxide precipitation in toxic areas of a wetland receiving trace element-enriched leachate from phosphate mine waste rock from the Permian Phosphoria Formation. The original source of the wetland Fe oxides is pyrite in the waste rock dumps. Tuttle et al. (2014a) found that incipient weathering of Mancos Shale during groundwater level lowering resulted in oxidation of pyrite and organic matter producing iron oxides and gypsum in the unsaturated, weathered shale formations found on the landscape today. Enrichment of Se was observed in laterally persistent Fe oxide layers as was presumed to be from selenite sorption onto the Fe oxides that formed during fluctuating redox conditions at the water table. Thus, in three different marine-origin sedimentary formations in the Interior West deposited in three different geologic time periods (Eocene Green River Formation at Pariette Draw, UT, Permian Phosphoria Formation in southeast ID, and Cretaceous Mancos Shale in the Colorado River Basin, iron mineral (pyrite) weathering and subsequent formation of hydrous Fe oxides have played an important role in release (during weathering) and attenuation (sorption) of Se chemical species.

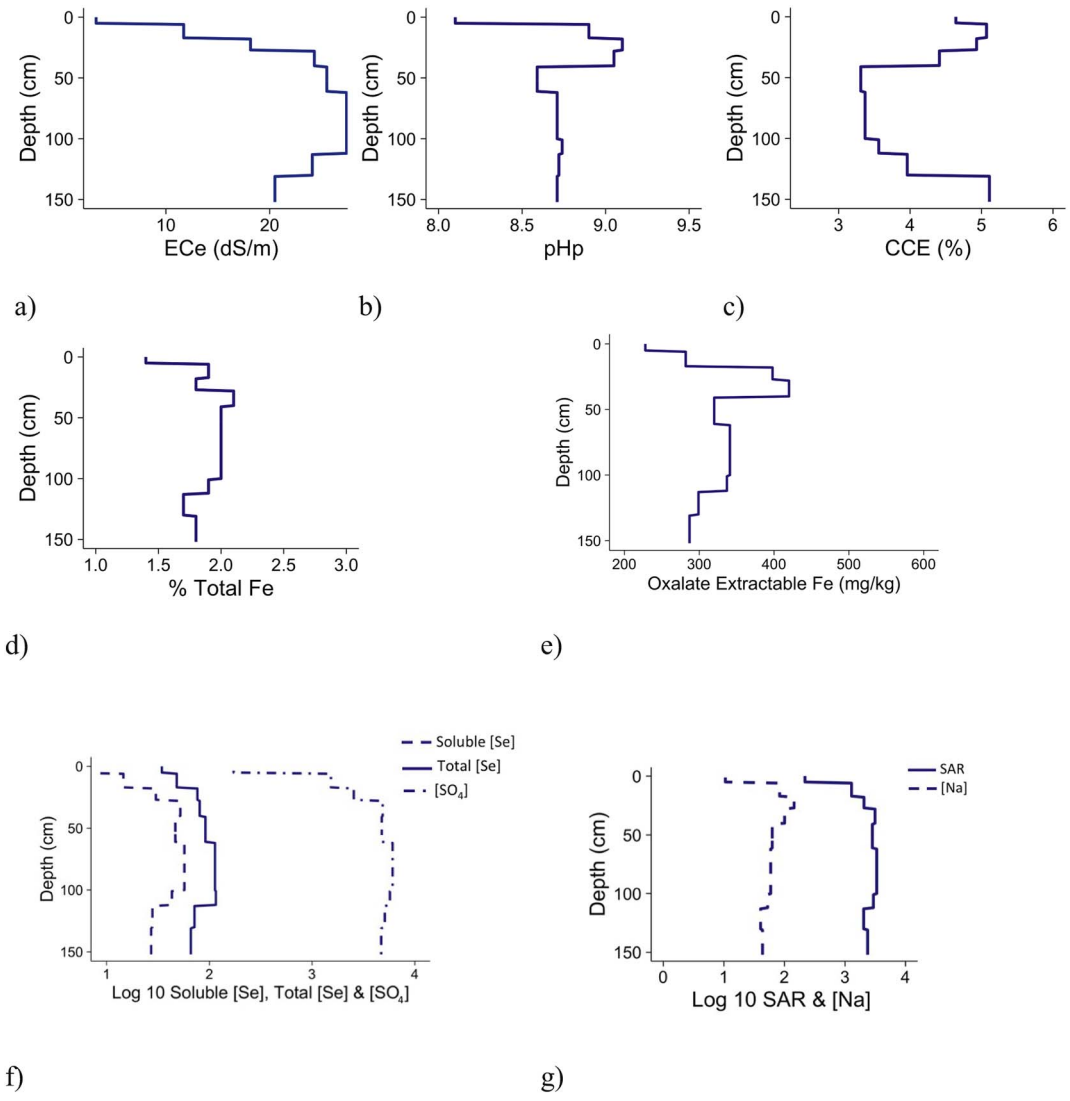

Fig. 4. Relationship to soil depth of wetland profile's chemical properties: a) electrical conductivity (dS/m), b) pH of extract paste, c) Calcium Carbonate Equivalent (%), d) Total Fe (%), e) Oxalate Extractable Fe (mg/kg), f) Log 10 transformation total [Se] (μg/kg), soluble [Se] (μg/kg) and [SO_4] (mg/kg), and g) Log 10 transformation SAR and [Na] (mg/kg).

The patterns in Figs. 4 and 5 gave valuable insight into effects of translocation of soluble salts, and the mobilization of selenium in these soils. The upland soil had higher total Se levels (87 to 217 μg/kg) than the wetlands soil (48 to 139 μg/kg), and both soils had a lower value than 440 μg/kg, which is the estimated mean total Se content of soils worldwide (Kabata-Pendias, 2011). Soluble Se concentrations measured in the saturated paste extracts for the each of the soil horizons differed between the two soils. In the upland soil, soluble Se could be detected only in the deepest horizons (86 to 154 cm) and ranged from 5.54 to 15.12 μg/kg, whereas in the wetlands soil soluble Se was present in all of the horizons, except the 6-cm surface horizon and ranged from 14.6 to 57.1 μg/kg. The wetlands profile had two to four times higher soluble Se concentrations than the upland profile (Table 2, Fig. 4f and f). The lack of intense and prolonged reducing conditions allow for Se to become oxidized. Oxidized Se became soluble and translocated from lower horizons to the Byz horizons in the wetland soil. Although the total Se concentrations measured in the wetland soil were nearly half that of the upland soil, a much greater proportion (21 to 52%) of the Se was soluble and thus bioavailable in the wetlands soil (Table 2). This also resulted in Se_e/Se_{Total} ratio about an order magnitude higher than the upland soil (Table 2). Thus, irrigation history has played a major role in Se mobilization. Tuttle et al. (2014b) found that during irrigation, salinity and Se loads from Mancos Shale increased 26% and 57% of the Uncompahgre River load, respectively. During 100 years of irrigation history, seven times more Se has been removed from agricultural soil than what was lost from natural landscapes during the entire period of pedogenesis. This same Se mobilization scenario is playing out in the Pariette Draw and wetlands area.

In contrast, soluble salts concentrations increased with depth in the upland soil due to infiltration of water and dissolution and leaching of salts to lower horizons (Fig. 5a) (Berger and Cooke, 1997). Several researchers have reported similar differences in soluble salts as a result of changes in water table as well as season. Berger and Cooke (1997) examined three similar alluvial fans in salar basins of northern Chile. The calcium sulfate distribution and other soluble salts were influence by a combination of groundwater, surface flow and wind (Berger and Cooke, 1997). Eghbal et al. (1989) investigated an alluvial fan in Carrizo Plain, California, where the overall salt concentrations were highest in the lower part of the profile away from Soda Lake due to leaching. The profiles closer to Soda Lake had higher salt concentrations towards the surface due to movement of groundwater (Eghbal et al., 1989).

Despite some association of Se with the Fe oxide fraction, primarily in the upland soil, Se movement in both soils is largely related to soil hydrology and salt movement. We surmise that soluble Se was most likely regulated by the solubility of a sodium selenite-sulfate

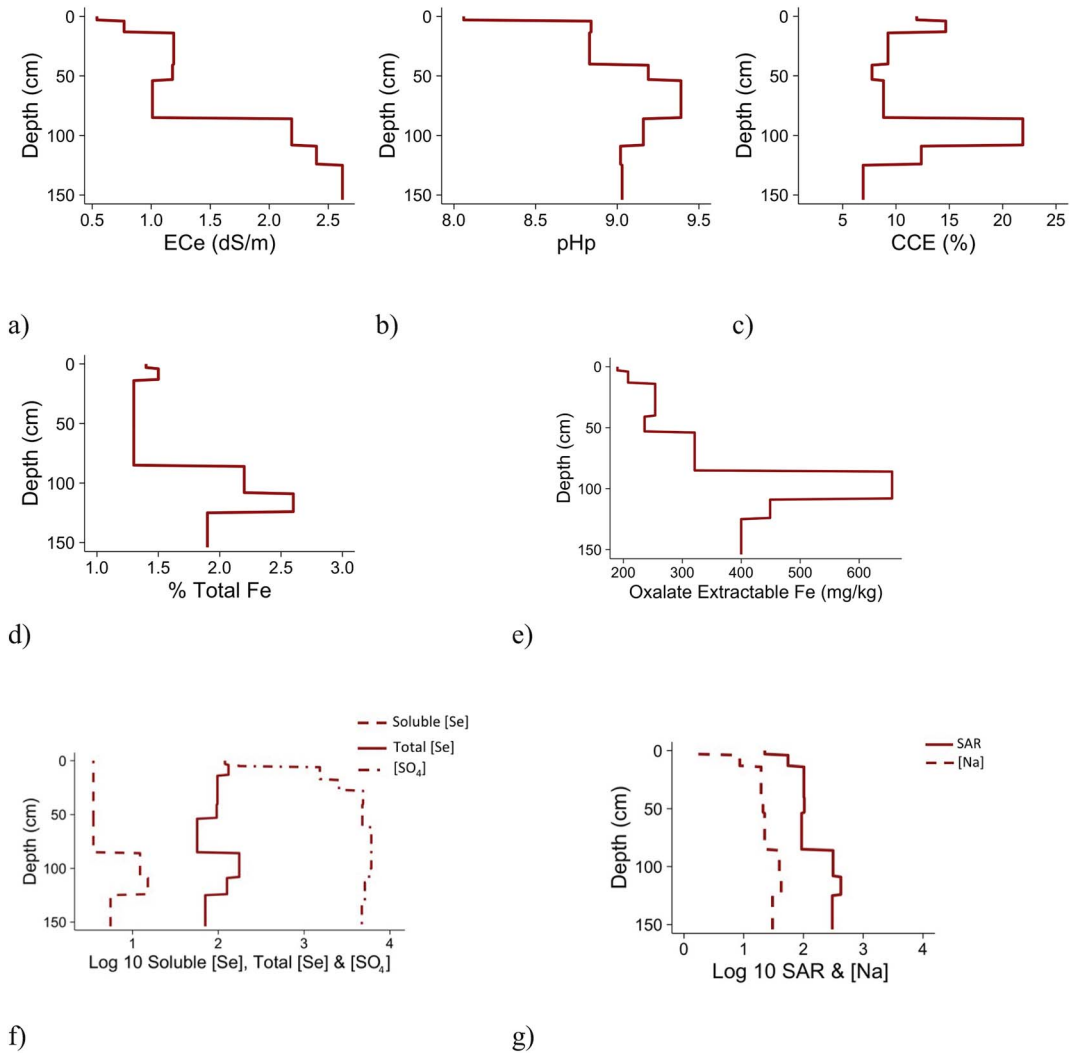

Fig. 5. Relationship to soil depth of upland profile's chemical properties: a) electrical conductivity (dS/m), b) pH of extract paste, c) Calcium Carbonate Equivalent (%), d) Total Fe (%), e) Oxalate Extractable Fe (mg/kg), f) Log 10 transformation total [Se] (μg/kg), soluble [Se] (μg/kg) and [SO_4] (mg/kg), and g) Log 10 transformation SAR and [Na] (mg/kg).

coprecipitate. The relatively low concentration of Se in the Pariette Wetlands soil indicates that Se is unlikely to form a discrete mineral phase thus it forms a coprecipitate with sulfate. The soil of Pariette Wetlands does not appear to be the source of Se that is negatively impacting wildlife in the wetlands. Nor were soil Se levels high enough to result in significant Se bioaccumulation from plants growing in these soils, or to the organisms that feed on them. The high soil salinity levels in the wetlands would have a greater impact on vegetative growth than Se. The high soluble sulfate content in the wetlands soils would inhibit Se uptake by plants (Mackowiak and Amacher, 2008). Most likely it is the exposure of water containing elevated levels of Se flowing through the wetlands that is the source of Se negatively impacting local wildlife.

4. Conclusions

Significant physical and chemical properties of the upland and wetlands soils differ as a result of alteration of the water table due to irrigation return water. Soluble Se concentrations were associated with

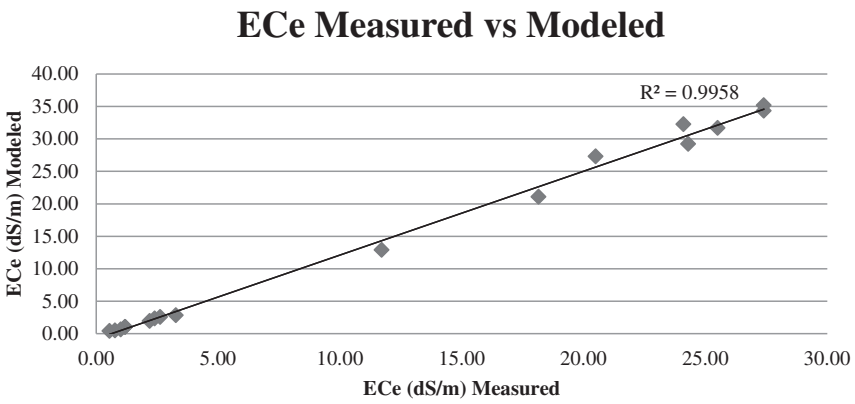

Fig. 6. Measured and molded ECe (dS/m) of paste extracts of upland and wetland soils were compared. Modeled ECe was calculated using PHREEQC (Parkhurst and Appelo, 2013) ionic strength output data for both soil profiles divided by Griffin and Jurinak (1973) activity coefficient (0.0127).

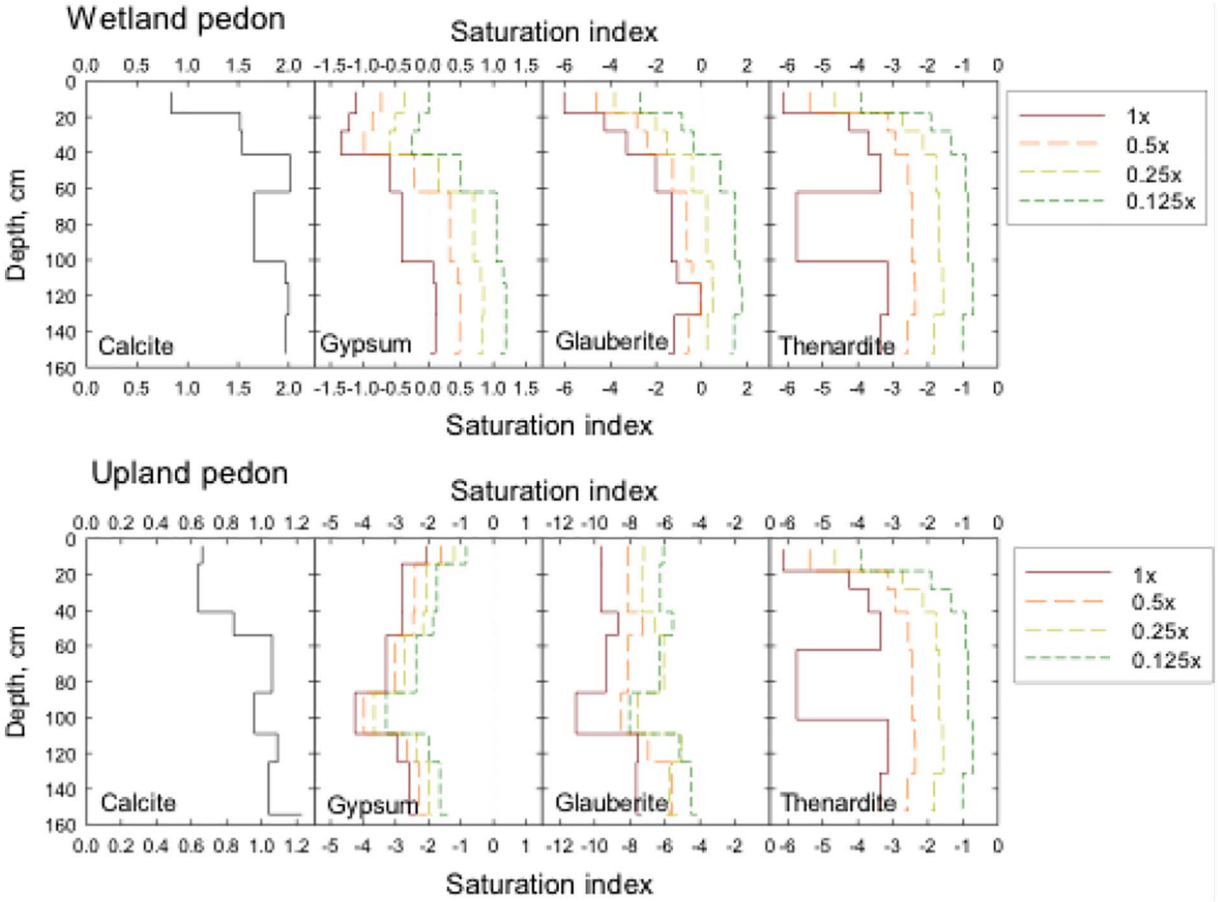

Fig. 7. Saturation indices (SI) from PHREEQC modeling of minerals in saturation extracts of soils from Pariette Draw, Utah. SI = 0 are saturated (equilibrium); SI < 0 are undersaturated; and SI > 0 are supersaturated..

soluble salts distribution, and to a lesser extent with Fe oxide distribution. Soluble salts levels were more than one order of magnitude greater in the wetlands profile than the upland profile. It appears that hydrology of the Pariette Draw is regulating the solubility of Se, sulfate and Fe within the soils profiles. Capillary migration was responsible for the translocation and accumulation of salts in the upper horizons (Byz horizons; 28 to 131 cm) of the wetlands soil, while lack of soluble salt and the distribution of CCE in the upland soil reflected downward translocation, typical of soils formed in arid climates. Within the Byz horizons of the wetlands soil, soluble salts were composed mostly of sulfates. Gypsum solubility regulated sulfate levels within the Byz horizons. Surface salt crusts within the wetlands soil were identified as thenardite (XRD and geochemical modeling). We surmised that soluble Se was most likely regulated by the solubility of a mixed sodium selenite-sulfate coprecipitate. It appears that the relatively low concentration of Se in the Pariette Wetlands soil was not the source and cause of Se responsible for adversely affecting wildlife in the wetlands. Instead, it is the exposure of water containing an elevated level of Se flowing through the wetlands that most likely is the source of Se negatively impacting animals.

Acknowledgements

The U.S. Bureau of Land Management (BLM #L09AC15859) financially supported this study. The authors are grateful to Darren Williams (USBLM Manager of Pariette Wetlands) and Sandy Wingert (UDEQ/DWQ Watershed Specialist) for their support and assistance.

References

Amrhein, C., Zahow, M.F., Suarez, D.L., 1993. Calcite supersaturation in soil suspensions. Soil Sci. 156 (3), 163–170.
Azaizeh, H.A., Salhani, N., Sebesvari, Z., Emons, H., 2003. The potential of rhizosphere microbes isolated from a constructed wetland to biomethylate selenium. J. Environ. Qual. 32 (1), 55–62.
Berger, I.A., Cooke, R.U., 1997. The origin and distribution of salts on alluvial fans in the Atacama desert, northern Chile. Earth Surf. Process. Landf. 22 (6), 581–600.
Boettinger, J.L., Richardson, J.L., 2001. Saline and wet soils of wetlands in dry climates. In: Richardson, J.L., Vepraskas, M.J. (Eds.), Wetland Soils: Genesis, Hydrology, Landscapes, and Classification. CRC Press, Boca Raton, FL, pp. 383–390.
Chapman, P.M., Adams, W.J., Brooks, M.L., Delos, C.G., Luoma, S.N., Maher, W.A., Ohlendorf, H.M., Presser, T.S., Shaw, D.P., 2010. Ecologial Assessmentt of Selenium in the Aquaitc Environment. CRC Press, Boca Raton, Florida.
Dzombak, D.A., Morel, F.M.M., 1990. Surface Complexation Modeling: Hydrous ferric oxide. John Wiley & Sons, New York (393 pp.).
Eghbal, M.K., Southard, R.J., Whittig, L.D., 1989. Dynamics of evaporite distribution in soils on a fan-playa transect in the Carrizo Plain, California. Soil Sci. Soc. Am. J. 53 (3), 898–903.
Fike, R.E., Phillips II, H.B., 1983. A nineteenth century Ute burial from northeast Utah. In: U.S.O.o.B.o.L. Management (Ed.), Symposium: Sixteenth Annual Meeting of Society for Historical Archaeology, Denver, Colorado.
Fonnesbeck, B.B., Boettinger, J.L., Lawley, J.R., 2013. Improving a simple pressure-calcimeter method for inorganic carbon analysis. Soil Sci. Soc. Am. J. 77, 1553–1562.
Frankenberger Jr., W.T., Engberg, R.A., 1998. Environmental Chemistry of Selenium. Marcel Dekker, Inc, New York, New York.
Goldberg, S., 2011. Chemical equilibrium and reaction modeling of arsenic and selenium in soils. In: Selim, H.M. (Ed.), Dynamics and Bioavailability of Heavy Metals in the Rootzone. CRC Press, Boca Raton, FL, pp. 65–92.
Griffin, B.A., Jurinak, J.J., 1973. Estimation of activity coefficients from the electrical conductivity of natural aquatic systems and soil extracts. Soil Sci. 116 (1), 26–30.
Hamilton, S.J., 2004. Review of selenium toxicity in the aquatic food chain. Sci. Total Environ. 326 (1–3), 1–31.
Hardie, L.A., Eugster, H.P., 1970. The evolution of closed-basin brines. Min. Soc. Am. Spe. Pap. 3, 273–290.
Hoffman, D.J., 2002. Role of selenium toxicity and oxidative stress in aquatic birds. Aquat. Toxicol. 57 (1–2), 11–26.

Kabata-Pendias, A., 2011. Trace Elements in Soils and Plants, fourth edition ed. CRC Press Taylor and Francis Groups, New York.
Laabs, B.J.C., Refsnider, K.A., Munroe, J.S., Mickelson, D.M., Applegate, P.J., Singer, B.S., Caffee, M.W., 2009. Latest Pleistocene glacial chronology of the Uinta Mountains: support for moisture-diven asychrony of last deglaciation. Quat. Sci. Rev. 28, 1171–1187.
Leishman, G.W., Fish, R.H., Lewis, R.J., 2003. Soil Survey of Uintah Area, Utah - Parts of Daggett, Grand, and Uintah Counties. In: U.S.D.o.A.N.R.C. Service (Ed.), Salt Lake City, Utah.
Lemly, A.D., 1985. Toxicology of selenium in a freshwater reservoir: implications for environmental hazard evaluation and safety. Ecotoxicol. Environ. Saf. 10, 314–338.
Lemly, A.D., 2002. Selenium Assessment in Aquatic Ecosystems: A Guide for Hazard Evaluation and Water Quality Criteria. Springer, New York.
Mackowiak, C.L., Amacher, M.C., 2008. Soil sulfur amendments suppress selenium uptake by alfalfa and western wheatgrass. J. Environ. Qual. 37, 772–779.
Maher, W., Roach, A., Doblin, M., Fan, T., Foster, S., Garrett, R., Moller, G., Oram, L., Wallschlager, D., 2010. Environmental sources, speciation, and partitioning of selenium. In: Chapman, P.M., Adams, W.J., Brooks, M.L., Delos, C.G., Luoma, S.N., Maher, W., Ohlendorf, H.M., Presser, T.S., Shaw, D.P. (Eds.), Ecological Assessment of Selenium in the Aquatic Environment. CRC Press, New York, pp. 47–92.
Naftz, D.L., Yahnke, J., Miller, J., Noyes, S., 2005. Selenium mobilization during a flood experiment in a contaminated wetland; Stewart Lake waterfowl management area, Utah. Appl. Geochem. 20 (3), 569–585.
Naftz, D.L., Bullen, T.D., Stolp, B.J., Wilkowske, C.D., 2008. Utilizing geochemical, hydrologic, and boron isotopic data to assess the success of a salinity and selenium remediation project, Upper Colorado River Basin, Utah. Sci. Total Environ. 392 (1), 1–11.
Ohlendorf, H.M., 2002. The birds of Kesterson Reservoir: a historical perspective. Aquat. Toxicol. 57 (1–2), 1–10.
Ohlendorf, H.M., Hoffman, D.J., Saiki, M.K., Aldrich, T.W., 1986. Embryonic mortality and abnormalities of aquatic birds: apparent impacts of selenium from irrigation drainwater. Sci. Total Environ. 52 (1–2), 49–63.
Ohlendorf, H.M., Hothem, R.L., Aldrich, T.W., 1988a. Bioaccumulation of Selenium by Snakes and Frogs in the San-Joaquin Valley, California. Copeia (3), 704–710.
Ohlendorf, H.M., Kilness, A.W., Simmons, J.L., Stroud, R.K., Hoffman, D.J., Moore, J.F., 1988b. Selenium toxicosis in wild aquatic birds. J. Toxicol. Environ. Health 24 (1), 67–92.
Parkhurst, D.L., Appelo, C.A.J., 2013. Description of Input and Examples for PHREEQC Version 3—A Computer Program for Speciation, Batch-reaction, One-dimensional Transport, and Inverse Geochemical Calculations: U.S. Geological Survey Techniques and Methods, Book 6, Chap. A43. 497 pp., Available only at http://pubs.usgs.gov/tm/06/a43/.
Peltz, L.A., Waddell, B., 1991. Physical, Chemical, and Biological Data for Detailed Study of Irrigation Drainage in the Middle Green River Basin, Utah 1988–89, With Selected Data for 1982–87. pp. 91–530.
Pollard, J., Cizdziel, J., Stave, K., Reid, M., 2007. Selenium concentrations in water and plant tissues of a newly formed arid wetland in Las Vegas, Nevada. Environ. Monit. Assess. 135 (1–3), 447–457.
Presser, T.S., 1994. The Kesterson effect. Environ. Manag. 18 (3), 437–454.
Presser, T.S., Sylvester, M.A., Low, W.H., 1994. Bioaccumulation of selenium from natural geologic sources in western states and its potential consequences. Environ. Manag. 18 (3), 423–436.
Prono, L., 2008. Utah climate center. In: Encyclopedia of Global Warming and Climate Change. SAGE Publications, Inc., Thousand Oaks, CA.
Ross, G.J., Wang, C., 1993. Chapter 25: Extractable Al, Fe, Mn, and Si. In: Carter, M.R. (Ed.), Soil Sampling and Methods of Analysis. CRC Press Inc., Boca Raton, Florida.
Rowland, R.C., Stephens, D.W., Waddell, B., Naftz, D.L., 2003. Selenium Contamination and Remediation at Stewart Lake Waterfowl Management Area and Ashley Creek, Middle Green River Basin, Utah. Fact Sheet - U. S. Geological Survey. pp. 6.
Seiler, R.L., 1995. Prediction of areas where irrigation drainage may induce selenium contamination of water. J. Environ. Qual. 24 (5), 973–979.
Seiler, R.L., Skorupa, J.P., Naftz, D.L., Nolan, B.T., 2003. Irrigation-induced Contamination of Water, Sediment, and Biota in the Western United States-Synthesis of Data From the National Irrigation Water Quality Program. pp. 1655.
Soil Survey Staff, 2009. Soil Survey Field and Laboratory Methods Manual. USDA-Natural Resources Conservation Service, Lincoln, NE.
Soil Survey Staff, 2010. Keys to Soil Taxonomy, 11th ed. USDA-Natural Resources Conservation Service, Washington D.C.
de Souza, M.P., Huang, C.P.A., Chee, N., Terry, N., 1999. Rhizosphere bacteria enhance the accumulation of selenium and mercury in wetland plants. Planta 209 (2), 259–263.
Stephens, D.W., Waddell, B., Miller, J.B., 1988. Reconnaissance Investigation of Water Quality, Bottom Sediment, and Biota Associated With Irrigation Drainage in the Middle Green River Basin, Utah 1986–87. In: U.S.G. Surv (Ed.), Salt Lake City, Utah.
Stephens, D.W., Waddell, B., Peltz, L.A., Miller, J.B., 1992. Detailed Study of Selenium and Selected Elements in Water, Bottom Sediment, and Biota Associated With Irrigation Drainage in the Middle Green River Basin, Utah 1988–90. In: U.S.G. Surv (Ed.), Salt Lake City, Utah.
Stillings, L.L., Amacher, M.C., 2004. Selenium attenuation in a wetland formed from mine drainage in the Phosphoria Formation, southeast Idaho. In: Hein, J.R. (Ed.), Life Cycle of the Phosphoria Formation: From Deposition to Post-mining Environment. Elsevier B.V., Amsterdam, The Netherlands, pp. 467–482.
Stokes, W.L., 1986. Geology of Utah. Museum of Natural History and Utah Geological and Mineral Survey. Department of Natural Resource, Salt Lake City.
Taggert Jr., J.E., 2002. Analytical method for chemical analysis of geologic and other materials. In: U.G. Surv. (Ed.), US Geol. Surv.
Tanji, K., Lauchli, A., Meyer, J., 1986. Selenium in the San-Joaquin Valley - a challenge to western irrigation. Environment 28 (6), 6–39.
Tuttle, M.L.W., Fahy, J.W., Elliott, J.G., Grauch, R.I., Stillings, L.L., 2014a. Contaminants from Cretaceous black shale: I. Natural weathering processes controlling contaminant cycling in Mancos Shale, southwestern United States, with emphasis on salinity and selenium. Appl. Geochem. 46, 57–71.
Tuttle, M.L.W., Fahy, J.W., Elliott, J.G., Grauch, R.I., Stillings, L.L., 2014b. Contaminants from cretaceous black shale: II. Effect of geology, weathering, climate, and land use on salinity and selenium cycling, Mancos Shale landscapes, southwestern United States. Appl. Geochem. 46 (0), 72–84.
U. S. EPA, 2014. Draft Aquatic Life Water Criteria for Selenium – 2004. In: Office of Water Office of Science and Technology (Ed.), Washington, D.C.
Wingert, S., Adams, C., 2011. TMDLs for Total Dissolved Solids, Selenium, and Boron in the Pariette Draw Watershed. U.D.o.E.Q.D.o.W. Quality (Ed.), Salt Lake City, Utah.
Winkel, L.H.E., Johnson, C.A., Lenz, M., Grundl, T., Leupin, O.X., Amini, M., Charlet, L., 2012. Environmental selenium research: from microscopic processes to global understanding. Environ. Sci. Technol. 46 (2), 571–579.
Zasoski, R.J., Burau, R.G., 1977. Rapid nitric-perchloric acid digestion method for multi-element tissue analysis. Commun. Soil Sci. Plant Anal. 8 (5), 425–436.